Proc. Estonian Acad. Sci. Phys. Math., 1995, 44, 2/3, 297–307
https://doi.org/10.3176/phys.math.1995.2/3.19

POLARONS IN THE TWO-DIMENSIONAL HOLSTEIN-*t*-*J* MODEL

Jörg SABCZYNSKI[a], Alexei SHERMAN[b], and Michael SCHREIBER[c]

[a] Institut für Physikalische Chemie, Johannes Gutenberg-Universität Mainz (University of Mainz), Jakob Welder-Weg 11, D-55099 Mainz, Deutschland (Germany)
[b] Eesti Teaduste Akadeemia Füüsika Instituut (Institute of Physics, Estonian Academy of Sciences), Riia 142, EE-2400 Tartu, Eesti (Estonia)
[c] Institut für Physik, Technische Universität Chemnitz-Zwickau (Technical University of Chemnitz-Zwickau) D-09107 Chemnitz, Deutschland (Germany)

Received 30 August 1994, accepted 17 April 1995

Abstract. To describe the dynamics of holes in CuO_2 planes of high-T_c superconductors we analyse the two-dimensional *t*-*J* model supplemented with the interaction of holes with nonpolar optical phonons. Elementary excitations of this model are treated nonadiabatically within the spin–wave approximation on an infinite square lattice by means of an iterative Lanczos algorithm. For parameter values relevant for high-T_c superconductors we have found a sharp crossover in the ground state from a nearly free excitation for small hole–phonon coupling to a self-trapped excitation for large hole–phonon coupling. In the vicinity of this crossover coexistence of these two types of states and ferron–phonon complexes has been found. We also analyse the dependence of the critical hole–phonon coupling strength on the exchange constant *J*.

Key words: high-T_c superconductivity, *t*-*J* model, polarons.

1. INTRODUCTION

The discovery of high-temperature superconductivity [1] has led to intense experimental and theoretical studies. A theory describing perovskite-like superconductors should include their most important properties, as there are the strong electron correlations and a quasi-two-dimensional band structure. It is usually believed that superconductivity takes place in copper-oxide planes which are a common structural element of most high-T_c materials. Conduction in these planes is mainly due to hole-like charge carriers introduced by doping, although there are also examples of electron-doped systems. It has been suggested that the two-dimensional Hubbard model can describe the charge carrier transport in the CuO_2 planes of high-T_c cuprate superconductors [2]. The most realistic model of this kind is a three-band Hubbard model taking into account the Cu-$d_{x^2-y^2}$ and the O-$p_{x,y}$ orbitals of copper-oxide planes [3]. In the limit

of large electron correlations and therefore large Hubbard repulsion this model can be mapped onto the t-J model [4] on a square lattice. In the case of hole doping the Hilbert space is restricted to states without doubly occupied lattice sites. Electron correlations are transformed into an antiferromagnetic interaction between electrons on neighbouring sites. Without doping, i. e. for exactly one electron per lattice site, this model reduces to a spin-1/2 Heisenberg model. The ground state of the Heisenberg model cannot be described exactly for large lattices, therefore such approximations or numerical methods as MC simulations [5] must be used. Spin–wave approximation yields surprisingly accurate results, as can be shown by comparison with MC results [6]. At low temperatures undoped and low-doped samples of perovskite superconductors are antiferromagnetically ordered [7], so the usage of spin–wave approximation can also be justified by experiment.

A number of unusual properties of high-T_c materials has led to a supposition that a purely electronic mechanism of the Cooper pairing plays the main role in a superconducting transition. Nevertheless, there are a number of experimental evidences that the influence of hole–phonon interaction cannot be neglected for a proper description of the transport properties of these crystals (for reviews, see e.g. [8, 9]). For example, a small but nonzero isotope effect [10], anomalously strong changes in the lattice dynamics at the superconducting transition [11, 12], singularities of the quadrupole frequency in NQR experiments [8, 13], which are especially sensitive to changes in field gradients due to local deformations, or the correlation between T_c and small low-temperature lattice distortions [14] show the important role played by the lattice in high-T_c materials. As possible mechanisms of the hole–phonon coupling the interaction with in-plane or apical oxygen modes has been considered (e.g. in [15–17]). Because of heavy masses of charge carriers and low carrier density, the Fermi energy in cuprate oxides is unusually low. Thus, the adiabatic approximation which requires that the phonon frequency be much smaller than the Fermi energy, is no longer justified (see, e.g. [18] and references therein) and the phonon modes must be taken into account nonadiabatically.

To understand the superconducting properties, the knowledge of the normal state is essential. Therefore the first step should be the investigation of a single hole in a copper-oxide plane, which is equivalent to the limit of low doping. Of special interest is whether the hole has a polaronic character and whether there exists a more or less sharp transition from a free to a self-trapped hole if the electron–phonon coupling is increased.

In this paper, to describe the dynamics of a single hole we use the Holstein-t-J Hamiltonian which includes a linear coupling of the hole density to effective local optical phonon modes. This Hamiltonian can be derived from the well-known Peierls–Hubbard Hamiltonian in the limit of large Hubbard repulsion [19]. Low-lying excitations of the model are investigated for the parameters presumably realized in La_2CuO_4. To calculate bound hole–magnon–phonon states, we use the spin–wave approximation [20–22] and an iterative Lanczos algorithm [23, 24].

2. MODEL AND CALCULATION PROCEDURE

The Holstein-*t*-*J* Hamiltonian for a square lattice as considered in this paper can be written in the form [19] ($\hbar = 1$)

$$H = H_{t-J} + H_{h-ph} + H_{ph},$$

$$H_{t-J} = -tP \sum_{\mathbf{ma}\sigma} c^{\dagger}_{\mathbf{m}+\mathbf{a},\sigma} c_{\mathbf{m}\sigma} P + \frac{J}{2} \sum_{\mathbf{ma}} \mathbf{s}_{\mathbf{m}+\mathbf{a}} \cdot \mathbf{s}_{\mathbf{m}}, \tag{1}$$

$$H_{h-ph} = \sqrt{S\Omega} \sum_{\mathbf{m}} (1 - n_{\mathbf{m}}) (B^{\dagger}_{\mathbf{m}} + B_{\mathbf{m}}),$$

$$H_{ph} = \Omega \sum_{\mathbf{m}} B^{\dagger}_{\mathbf{m}} B_{\mathbf{m}}.$$

Here $H_{t\text{-}J}$ is the *t*-*J* Hamiltonian, t and J are the bare hopping matrix element and the superexchange constant, respectively, and P is the projection operator onto the subspace of the Hilbert space without doubly occupied lattice sites. The Fermi operator $c^{\dagger}_{\mathbf{m}\sigma}$ creates an electron on the site $\mathbf{m} = (m_x, m_y)$ of the square lattice with the spin label σ ($\sigma = \pm 1$). The spin operator $\mathbf{s}_{\mathbf{m}}$ consists of $s^z_{\mathbf{m}} = \sum_{\sigma} \sigma c^{\dagger}_{\mathbf{m}\sigma} c_{\mathbf{m}\sigma}/2$ and $s^{\sigma}_{\mathbf{m}} = s^x_{\mathbf{m}} + i\sigma s^y_{\mathbf{m}} = c^{\dagger}_{\mathbf{m}\sigma} c_{\mathbf{m},-\sigma}$. The summation over $\mathbf{a}$ is carried out over nearest neighbour sites only. H_{ph} describes local optical phonon modes with the frequency Ω and $B^{\dagger}_{\mathbf{m}}$ creates a phonon at the site $\mathbf{m}$. $n_{\mathbf{m}} = \sum_{\sigma} c^{\dagger}_{\mathbf{m}\sigma} c_{\mathbf{m}\sigma}$ is the electron density at the site $\mathbf{m}$ and $H_{h\text{-}ph}$ displays a Holstein coupling of the hole density $(1 - n_{\mathbf{m}})$ to local phonon modes, where S is the hole–phonon coupling parameter. Terms of the static hole–hole interaction resulting from the mapping procedure are constant for the considered one-hole states and have been omitted in Eq. (1) [25].

The spin–wave approximation, which has been shown to yield remarkably accurate results for the Heisenberg and the *t*-*J* model [6, 25–27], is introduced with the help of the following formulas [22]:

$$s^{+1}_{\mathbf{m}} = \Phi_{\mathbf{m}} b_{\mathbf{m}} P^{+1}_{\mathbf{m}} + b^{\dagger}_{\mathbf{m}} \Phi_{\mathbf{m}} P^{-1}_{\mathbf{m}}, \quad s^{-1}_{\mathbf{m}} = (s^{+1}_{\mathbf{m}})^{\dagger},$$

$$s^z_{\mathbf{m}} = e^{i\Pi \cdot \mathbf{m}} \left(\frac{n_{\mathbf{m}}}{2} - b^{\dagger}_{\mathbf{m}} b_{\mathbf{m}} \right) \tag{2}$$

with $\Phi_{\mathbf{m}} = \sqrt{1 - b^{\dagger}_{\mathbf{m}} b_{\mathbf{m}}}$, $P^{\sigma}_{\mathbf{m}} = \frac{1}{2}(1 + \sigma e^{i\Pi \cdot \mathbf{m}})$, $\Pi = \left(\frac{\pi}{a}, \frac{\pi}{a} \right)$.

Here a is the lattice constant and the spin–wave operators $b_{\mathbf{m}}$ satisfy the commutation relations $\left[b_{\mathbf{m}_1}, b^{\dagger}_{\mathbf{m}_2}\right] = \delta_{\mathbf{m}_1,\mathbf{m}_2} n_{\mathbf{m}_1}$ and $\left[b_{\mathbf{m}_1}, b_{\mathbf{m}_2}\right] = 0$. The vacuum state for the spin–wave operators is one of the two classical Néel states, $|\mathcal{N}>: b_{\mathbf{m}}|\mathcal{N}> = 0$. The two possible Néel states are decoupled in the thermodynamic limit, thus it is sufficient to investigate only one of them.

After the substitution of Eqs. (2) into the Heisenberg part of $H_{t\text{-}J}$, the spin–wave approximation means the neglecting of the terms of the third and higher order in $b_{\mathbf{m}}$. The obtained quadratic form in $b_{\mathbf{m}}$ and $b^{\dagger}_{\mathbf{m}}$ can be diagonalized by the unitary transformation [22]

$$T = \exp\left[\sum_{\mathbf{k}} \alpha_{\mathbf{k}} (b_{\mathbf{k}} b_{-\mathbf{k}} - b^{\dagger}_{\mathbf{k}} b^{\dagger}_{-\mathbf{k}})\right] \text{ with } \alpha_{\mathbf{k}} = \frac{1}{8} \ln\left(\frac{1+\gamma_{\mathbf{k}}}{1-\gamma_{\mathbf{k}}}\right)$$

$$\text{and} \quad \gamma_{\mathbf{k}} = \frac{1}{4} \sum_{\mathbf{a}} e^{i\mathbf{k}\mathbf{a}}. \tag{3}$$

$b_{\mathbf{k}}$ and $b^{\dagger}_{\mathbf{k}}$ are the Fourier transforms of $b_{\mathbf{m}}$ and $b^{\dagger}_{\mathbf{m}}$, respectively. After this transformation the Hamiltonian H (see Eq. (1)) reads

$$\mathcal{H} = T^{\dagger} H T = t \sum_{\mathbf{mna}} \left[h_{\mathbf{m}+\mathbf{a}} h^{\dagger}_{\mathbf{m}} b_{\mathbf{m}-\mathbf{n}} (u_{\mathbf{n}+\mathbf{a}} + v_{\mathbf{n}}) + \text{h.c.}\right] +$$

$$+ \frac{J}{2} \sum_{\mathbf{mn}} \omega_{\mathbf{n}} b^{\dagger}_{\mathbf{m}} b_{\mathbf{m}+\mathbf{n}} + \Omega \sum_{\mathbf{m}} B^{\dagger}_{\mathbf{m}} B_{\mathbf{m}} + \sqrt{S\Omega} \sum_{\mathbf{m}} h^{\dagger}_{\mathbf{m}} h_{\mathbf{m}} (B^{\dagger}_{\mathbf{m}} + B_{\mathbf{m}}), \tag{4}$$

where $h^{\dagger}_{\mathbf{m}} = \sum_{\sigma} P^{\sigma}_{\mathbf{m}} c_{\mathbf{m}\sigma}$ creates a hole on the site $\mathbf{m}$. $u_{\mathbf{m}}$, $v_{\mathbf{m}}$, and $\omega_{\mathbf{m}}$ are the Fourier transforms of $\cosh(2\alpha_{\mathbf{k}})$, $-\sinh(2\alpha_{\mathbf{k}})$, and $4\sqrt{1-\gamma^2_{\mathbf{k}}}$, respectively. A more detailed derivation of Hamiltonian (4) can be found in [19, 22].

Since $u_{\mathbf{m}+\mathbf{a}} + v_{\mathbf{m}}$ and $\omega_{\mathbf{m}}$ decrease very rapidly with the increasing of $|\mathbf{m}|$, it is sufficient to keep only the components with $\mathbf{m} = (\pm a, 0), (0, \pm a)$ for $u_{\mathbf{m}+\mathbf{a}} + v_{\mathbf{m}}$ and those with $\mathbf{m} = (0,0), (\pm a, \pm a), (\pm 2a, 0), (0, \pm 2a)$ for $\omega_{\mathbf{m}}$ in the calculation; for symmetry reasons $\omega_{\mathbf{m}} = 0$ for $\mathbf{m} = (\pm a, 0)$, $(0, \pm a)$ and $u_{\mathbf{m}+\mathbf{a}} + v_{\mathbf{m}} = 0$ for $\mathbf{m} = (0,0)$.

Symmetries can be used to classify the eigenstates of the Hamiltonian. The eigenstates are characterized by the z component S_z of the total spin, the two-dimensional wave vector $\mathbf{k}$ and an irreducible representation of the corresponding wave-vector group. By a given set of these quantum numbers a subspace of the Hilbert space is determined. Within this

subspace the lowest eigenstate of the Hamiltonian can be determined with the help of the following modified iterative Lanczos procedure[22]: starting from an initial state $|i\rangle$ from one of the subspaces mentioned in each step of iteration, the procedure creates a final state $|f\rangle$ according to

$$\langle i|i\rangle = 1, \quad E_i = \langle i|\mathcal{H}|i\rangle, \quad V|f\rangle = (\mathcal{H} - E_i)\,|i\rangle. \tag{5}$$

V is the normalization constant which follows from $\langle f|f\rangle = 1$. Now the energy is minimized in the two-dimensional subspace spanned by $|i\rangle$ and $|f\rangle$ and the obtained state $|i'\rangle$ is used as the starting state in the next step of the Lanczos iteration. Since the iteration consists mainly in the action of the Hamiltonian $\mathcal{H}$ on $|i\rangle$, $|f\rangle$ has the same quantum numbers as $|i\rangle$. Thus the symmetry of the starting state is not changed during the iteration.

Bound hole–magnon–phonon states can be represented in the form

$$|s\rangle = \sqrt{\frac{2}{N}} \sum_{\sigma \mathbf{L}_\sigma} \sum_{\nu} \sum_{\mu} \sum_{\{\mathbf{n}_\nu\}} \sum_{\{\mathbf{m}_\mu\}} e^{i\mathbf{k}\mathbf{L}_\sigma} \frac{1}{\sqrt{\nu!\,\mu!}} D_s(\sigma, \nu, \mu, \{\mathbf{n}_\nu\}, \{\mathbf{m}_\mu\}) \times$$

$$\times B^\dagger_{\mathbf{L}_\sigma + \mathbf{m}_1} \ldots B^\dagger_{\mathbf{L}_\sigma + \mathbf{m}_\mu}\, b^\dagger_{\mathbf{L}_\sigma + \mathbf{n}_1} \ldots b^\dagger_{\mathbf{L}_\sigma + \mathbf{n}_\nu}\, h^\dagger_{\mathbf{L}_\sigma} |vac\rangle, \tag{6}$$

where $|s\rangle = |i\rangle$, $|i'\rangle$ or $|f\rangle$. $\mathbf{L}_\sigma$ labels the sites of the spin sublattice σ in the Néel state $|\mathcal{N}\rangle$, $|vac\rangle$ is the direct product of the phonon vacuum state and the Néel state. After substituting Eq. (6) into Eqs. (5), we obtain formulas showing the dependence of the expansion coefficients D_f of the final state $|f\rangle$ on the expansion coefficients D_i of the initial state $|i\rangle$ [22, 28]. These equations can be used for the numerical procedure.

Starting with an initial state with a finite number of nonzero coefficients D_i, the number of components of the states $|s\rangle$ grows rapidly during iteration. Therefore, in each step of iteration procedure (5) we restrict expansion (6) of $|i'\rangle$ to the j components with the largest amplitudes. In this work $j = 100$ is sufficient. After renormalization this restricted state is used as the initial state in the next step of Lanczos procedure (5). As follows from Eqs. (5), this modification as well as the original procedure gives an upper bound for the lowest eigenvalue of the energy at given quantum numbers if the projection of the starting state onto the ground one is nonzero (for more details see [22, 25]). Naturally, the special form of trial states (6) allows us to calculate only bound hole–phonon–magnon states (one-particle states) and not two-(or more)-particle scattering states.

3. RESULTS AND DISCUSSION

To determine the properties of cuprate superconductors it is necessary to first of all derive the values of the model parameters J, t, Ω, and S. The mapping procedure [12, 29] used to derive the t-J-Hamiltonian allows us to

estimate t and J from the known parameters of La_2CuO_4 [30, 31]. Estimations for t range from 0.3 to 0.4 eV and for J from 0.1 to 0.15 eV. Neutron scattering experiments [7] have confirmed this value of the superexchange constant J. The frequency Ω of local optical phonons can be measured by Raman and IR spectroscopy (see e.g. [9], for La_2CuO_4 Ω is in the range from 10 to 70 meV). Estimations of the hole–phonon coupling strength are still controversial, but it is believed that S is between $0.1t$ and t [17].

In the calculations reported here we used $J/t = 0.05$–1.0, $\Omega/t = 0.15$, and $S/t = 0$–7.5, which covers the range of the parameter space relevant for high-T_c superconductors.

To understand the Holstein-t-J model, the pure t-J model is an appropriate starting point. The energy spectrum of $H_{t\text{-}J}$ (see Eq. (1)) for a single hole consists of the energy bands characterized by definite values of S_z. Each of these bands forms the edge of a continuum of hole–magnon scattering states [20, 25]. For $J/t < 0.053$ the ground state has $S_z \geq 3/2$ and the hole is surrounded by a cloud of ferromagnetically ordered electron spins forming a so-called ferron [22, 25, 32]. In the range of the J/t investigated here the lowest one-hole band has $S_z = 1/2$. Its ground state has been found at the edge of the magnetic Brillouin zone at $\mathbf{k}_g = (\pm\pi/a, \pm\pi/a)$ and it is fourfold degenerate, while its maximum occurs at $\mathbf{k}=0$ [25]. Only for $J/t > 0.92$ the ground-state energy is given by the $S_z=1/2$ band in the entire Brillouin zone. For smaller J/t the lowest energy in the middle of the Brillouin zone is given by $S_z=3/2$. In this paper, we are mainly interested in the behaviour of the global ground state for the parameters relevant for copper oxides, thus, we restrict our investigation to the $S_z=1/2$ band only.

The influence of the hole–phonon coupling on the ground-state energy can be seen in Fig. 1 for the case of $J/t=0.3$ and $\Omega/t=0.15$. For $S=0$, the electronic system and the vibrational system are decoupled. For a small hole–phonon coupling S, the ground-state energy decreases slightly with the increasing of S and the number N_{ph} of the phonons escorting the hole increases, although N_{ph} is much smaller than one (see Fig. 1). In this region, the ground state still has the wave vector $\mathbf{k}=\mathbf{k}_g$. Its wave function is still similar to the wave function in the decoupled case. This behaviour is typical of a nearly free quasi-particle [33, 34].

The character of the ground state changes drastically near a critical value $S_c=1.4t$. Above S_c the ground-state energy decreases much faster and in the limit of large S it approaches $S + E_0$, where E_0 is a constant. For $S > S_c$ the number of phonons N_{ph} connected to the hole grows rapidly and is much larger than unity already for the S only slightly larger than S_c. In the limit of large S, N_{ph} approaches S/Ω, which indicates that the ground-state wave function is the phonon-relaxed localized state.

Our method allows us to consider not only the lowest state but also well-defined metastable states. If the starting state has a sufficiently large overlap with some metastable state, the Lanczos procedure will 'stick' in this state. We used two essentially different states as starting states: the mobile bare hole state and the localized phonon-relaxed state [35]. The results obtained indicate that near S_c the respective energetically higher state coexists with the lowest state as a well-defined metastable state (Fig. 2).

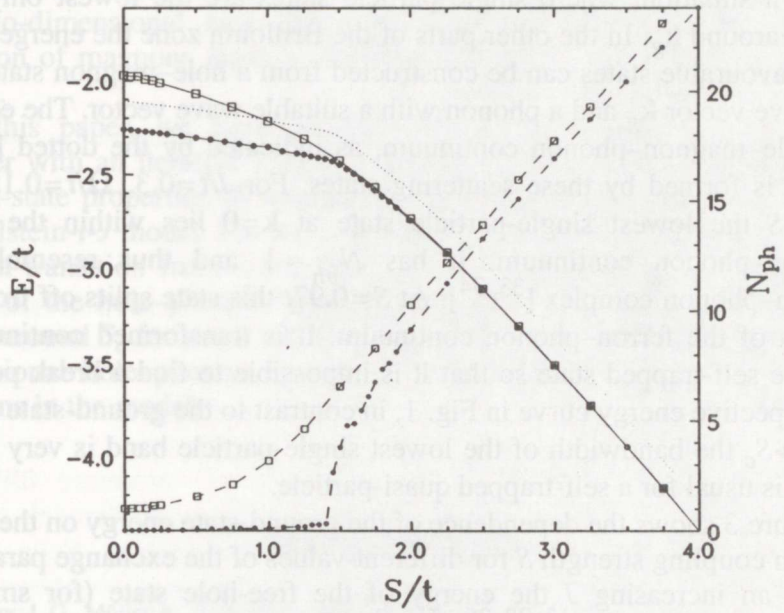

Fig. 1. The lowest energy E of bound hole–magnon–phonon states (solid lines, left scale) and the number of escorting phonons N_{ph} (dashed lines, right scale) for $\mathbf{k} = \mathbf{k}_g$ (•) and $\mathbf{k} = 0$ (□). $J/t = 0.3$, $\Omega/t = 0.15$. The hole–phonon continuum edge is shown by the dotted line.

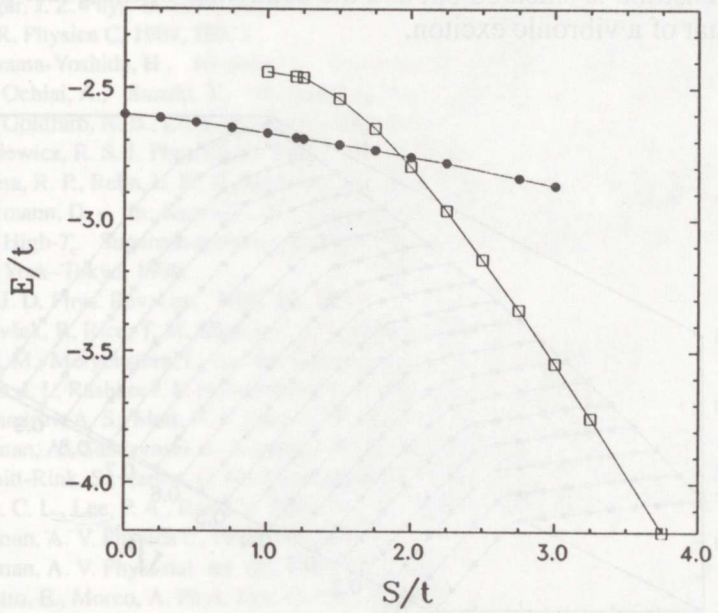

Fig. 2. Coexistence of self-trapped (□) and free-hole states (•) for $J/t = 0.1$ and $\Omega/t = 0.15$.

For $\mathbf{k} \neq \mathbf{k}_g$ the situation is different. The inclusion of optical phonons of the frequency Ω, which is sufficiently small (e.g. $J/t=0.3$, $\Omega/t=0.15$), yields a situation, where single particle states are the lowest only in a region around $\mathbf{k}_g$. In the other parts of the Brillouin zone the energetically most favourable states can be constructed from a hole–magnon state with the wave vector $\mathbf{k}_g$ and a phonon with a suitable wave vector. The edge of the hole–magnon–phonon continuum, as indicated by the dotted line in Fig. 1, is formed by these scattering states. For $J/t=0.3$, $\Omega/t=0.15$, and small S the lowest single-particle state at $\mathbf{k}=0$ lies within the hole–magnon–phonon continuum. It has $N_{ph} \approx 1$ and thus resembles an exciton–phonon complex [33, 34]. At $S=0.97t$ this state splits off from the bottom of the ferron–phonon continuum. It is transformed continuously into the self-trapped state so that it is impossible to find a break point in the respective energy curve in Fig. 1, in contrast to the ground-state curve. For $S>S_c$ the bandwidth of the lowest single-particle band is very small, which is usual for a self-trapped quasi-particle.

Figure 3 shows the dependence of the ground-state energy on the hole–phonon coupling strength S for different values of the exchange parameter J. For an increasing J the energy of the free-hole state (for small S) increases as expected [13, 22, 25] and the dependence on S becomes more pronounced. The ground-state energy in the self-trapped region of the parameter space depends only slightly on J. The critical hole–phonon coupling S_c and the size of the coexistence region decrease with increasing J. For $J/t \geq 0.7$ the coexistence region vanishes, i. e. the Lanczos procedure converges to the same final state independent of the starting state. The transition is smeared out and the behaviour of the quasi-particle resembles that of a vibronic exciton.

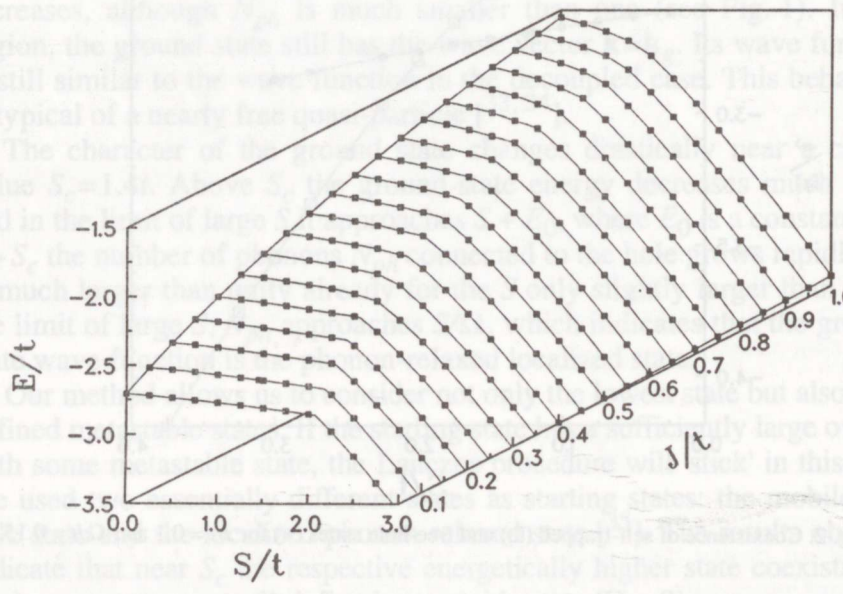

Fig. 3. Dependence of the ground-state energy E on S for different values of J/t.

In the hole–phonon system no coexistence of free and self-trapped states has been found in the two-dimensional case, but is expected to be inherent in the three-dimensional system [36]. The observed coexistence in the two-dimensional hole–phonon–magnon system indicates that the inclusion of magnons leads to essential changes in the properties of the system.

In this paper, we have shown that the spin–wave approximation together with an iterative Lanczos procedure allows us to determine the ground-state properties of weakly doped cuprate superconductors within the Holstein-*t-J* model. For the parameters relevant for La_2CuO_4 we have found a transition from a free-hole state to a self-trapped state at large values of the hole–phonon coupling parameter. Both states coexist in a region around S_c for small *J/t*. This behaviour, rather unusual for the two-dimensional hole–phonon system, is observed due to the inclusion of magnons in the model.

REFERENCES

1. Bednorz, J. G., Müller, K. A. Z. Phys., 1986, **64**, 189.
2. Anderson, P. W. Science, 1987, **235**, 1196.
3. Emery, V. J. Phys. Rev. Lett., 1987, **58**, 2794.
4. Zhang, F. C., Rice, T. M. Phys. Rev. B, 1988, **37**, 3759.
5. Reger, J. D., Young, A. P. Phys. Rev. B, 1988, **37**, 5978.
6. Huse, D. A. Phys. Rev. B, 1988, **37**, 2380.
7. Keimer, B., Belk, N., Birgeneau, R. G., Cassanho, A., Chen, C. Y., Greven, M., Kastner, M. A., Aharony, A., Endoh, Y., Erwin, R. W., Shirane, G. Phys. Rev. B, 1992, **46**, 14034.
8. Ranniger, J. Z. Phys. B, 1991, **84**, 167.
9. Feile, R. Physica C, 1989, **159**, 1.
10. Katayama-Yoshida, H., Hirooka, T., Oyamada, A., Okabe, Y., Takahashi, T., Sasaki, T., Ochiai, A., Suzuki, T., Mascarenhas, A. J., Pankove, J. I., Ciszek, T. F., Deb, S. K., Goldfarb, R. B., Li, Y. Physica C, 1988, **156**, 481.
11. Markiewicz, R. S. J. Phys. Cond. Matt., 1990, **2**, 6223.
12. Sharma, R. P., Rehn, L. E., Baldo, P. M., Liu, J. Z. Phys. Rev. Lett., 1989, **62**, 2869.
13. Brinkmann, D. – In: Kuzmany, H., Mehring, M., Fink, J. (eds.). Electronic Properties of High-T_c Superconductors and Related Compounds. Springer, Berlin–Heidelberg–New York–Tokyo, 1990.
14. Axe, J. D. Phys. Rev. Lett., 1989, **62**, 2751.
15. Prelovšek, P., Rice, T. M., Zhang, F. C. J. Phys. C, 1989, **20**, L229.
16. Frick, M., Morgenstern, I., von der Linden, W. Z. Phys. B, 1991, **82**, 339.
17. Mazin, I. I., Rashkeev, S. N., Savrasov, S. Y. Phys. Rev. B, 1990, **42**, 366.
18. Alexandrov, A. S., Mott, N. F. Supercond. Sci. Technol., 1993, **6**, 215.
19. Sherman, A., Sabczynski, J., Schreiber, M. Z. Phys. B, 1991, **84**, 343.
20. Schmitt-Rink, S., Varma, C. M., Ruckenstein, A. E. Phys. Rev. Lett., 1988, **60**, 2793.
21. Kane, C. L., Lee, P. A., Read, N. Phys. Rev. B, 1989, **39**, 6880.
22. Sherman, A. V. Physica C, 1990, **171**, 395.
23. Sherman, A. V. Phys. stat. sol. (b), 1985, **131**, 225.
24. Dagotto, E., Moreo, A. Phys. Rev. D, 1985, **31**, 865.
25. Sabczynski, J., Schreiber, M., Sherman, A. Phys. Rev. B, 1993, **48**, 543.
26. Marsiglio, F., Ruckenstein, A. E., Schmitt-Rink, S., Varma, C. M. Phys. Rev. B, 1991, **43**, 10882.
27. Sherman, A. V. Physica C, 1993, **211**, 329.

28. Sherman, A. V. J. Phys. A, 1987, **20**, 569.
29. Sherman, A. V. Phys. Rev. B, 1993, **47**, 11521.
30. Grilli, M., Castellani, C., Di Castro, C. Phys. Rev. B, 1990, **42**, 6233.
31. McMahan, A. K., Annett, J. F., Martin, R. M. Phys. Rev. B, 1990, **42**, 6268.
32. Schreiber, M., Sabczynski, J., Sherman, A. Phil. Mag., 1992, **65**, 881.
33. Sumi, H. J. Phys. Soc. Japan, 1974, **36**, 770; 1975, **38**, 825.
34. Sherman, A. V. Phys. stat. sol. (b), 1987, **141**, 151.
35. Sabczynski, J., Sherman, A., Schreiber, M. Phys. Lett. A, 1994, **195**, 231.
36. Rashba, E. I. – In: Rashba, E. I., Sturge, M. D. (eds.). Excitons. North-Holland, Amsterdam, 1982.

POLARONID ELEKTRON–FOONON-INTERAKTSIOONIGA TÄIENDATUD KAHEMÕÕTMELISES *t-J*-MUDELIS

Jörg SABCZYNSKI, Aleksei ŠERMAN, Michael SCHREIBER

On analüüsitud aukude dünaamikat kõrgtemperatuursete ülijuhtide CuO_2-kihtides kahemõõtmelise *t-J*-mudeli baasil, mida täiendab laengukandjate vastakmõju mittepolaarsete optiliste foononitega. Selle mudeli elementaarergastusi uuritakse lõpmatus ruutvõres ilma adiabaatilise lähenduseta, kasutades spinnlainete lähendust ja Lanczosi iteratsioonialgoritmi. Parameetrite intervallis, mis vastab kõrgtemperatuursetele ülijuhtidele, on leitud põhiseisundis järsk krossover nõrga augu–foononi vastakmõjuga kvaasivabalt ergastuselt tugeva vastakmõjuga iselokaliseerunud ergastusele. Krossoveri punkti läheduses on avastatud nende kahe ergastuse ja ferroon–foonon-kompleksi kooseksisteerimine. On analüüsitud augu–foononi vastakmõju kriitilise konstandi sõltuvust vahetuskonstandist *J*.

ПОЛЯРОНЫ В ДВУМЕРНОЙ *t–J*-МОДЕЛИ, ДОПОЛНЕННОЙ ЭЛЕКТРОН-ФОНОННЫМ ВЗАИМОДЕЙСТВИЕМ

Йорг САБЧИНСКИ, Алексей ШЕРМАН, Михаэль ШРАЙБЕР

Динамика дырок в CuO_2-плоскостях высокотемпературных сверхпроводников анализируется на основе двумерной *t–J*-модели, дополненной взаимодействием носителей с неполярными оптическими фононами. Элементарные возбуждения этой модели исследуются на бесконечной квадратной решетке без применения адиабатического приближения, но с использованием спин-волнового приближения и итерационного алгоритма Ланцоша. Для интервала параметров, соответствующего высокотемпературным сверхпроводникам, обнаружен резкий кроссовер основного состояния от почти-свободных возбуждений при слабом дырочно-фононном взаимодействии к автолокализованным возбуждениям при сильном

взаимодействии. В окрестности точки кроссовера обнаружено сосуществование этих двух типов возбуждений и феррон-фононных комплексов. Проанализирована зависимость критической константы дырочно-фононного взаимодействия от обменной константы J.